processes

MDPI

Article

Biosorption of Cd^{2+} from Water Using *Rhodotorula* sp. Immobilized on Rice Husk

Samantha Montserrat Ramírez-Sologuren [1], Ana Karen Ivanna Flores-Trujillo [2,*] and Refugio Rodríguez-Vázquez [2,*]

[1] Interdisciplinary Professional Unit of Biotechnology (UPIBI-IPN), Luis Enrique Erro Avenue, Zacatenco, Mexico City 07738, Mexico; sramirezs1800@alumno.ipn.mx
[2] Department of Biotechnology and Bioengineering, Center for Research and Advanced Studies of the National Polytechnic Institute (CINVESTAV-IPN), Instituto Politécnico Nacional Avenue, No. 2508, Zacatenco, Mexico City 07360, Mexico
* Correspondence: ivanna.flores@cinvestav.mx (A.K.I.F.-T.); rrodrig@cinvestav.mx (R.R.-V.)

Abstract

Cadmium (Cd^{2+}) is a potentially toxic element that is a health and environmental risk agent, especially when found in water bodies. The objective of this study was to evaluate the removal efficiency of untreated rice husk as a biosorbent and the yeast *Rhodotorula* sp., immobilized on the same fiber, for Cd^{2+} removal from an aqueous solution. Micrographs and biosorption assays were performed in batch systems, comparing the efficiency of the unmodified fiber and the fiber with the immobilized microorganism. The percentage of removal and the biosorption capacity were also determined, and the experimental data were analyzed using kinetic models and adsorption isotherms. The immobilization of the microorganism increased the Cd^{2+} (1 mg/L) removal efficiency to 99.79%, compared to untreated rice husk, which was removed to 92.99%; however, no difference was observed in the biosorption capacity of the untreated fiber (3.54 mg/g) versus the yeast-immobilized material (3.52 mg/g). Both materials fit better to the Sips model (R^2 = 0.9977–0.9989) and pseudo-second-order kinetics (R^2 = 0.9826–0.9944). The results suggest that knowing the Cd concentration is important for selecting the most suitable removal system; nevertheless, both alternatives could be used to remove this contaminant from water.

Keywords: potentially toxic elements; microorganisms; removal; cadmium; rice husk; biosorbent

1. Introduction

The impact of contaminants on water quality is of global interest, as they trigger a chain of effects within the ecosystem that alter its balance and dynamics, primarily through the mobilization of contaminants and the decrease of oxygen availability [1,2].

Among these contaminants, potentially toxic elements (PTEs) is a term used for heavy metals, the metalloid group, and other non-metals that, depending on their concentration, have a high degree of toxicity, persistence, bioaccumulation, and biomagnification in flora, fauna, and humans [3].

Cadmium (Cd) is one of these elements, characteristically non-biodegradable, non-essential, toxic, and with carcinogenic and teratogenic effects, which usually bioaccumulates in the human body [4,5]. Prolonged human exposure to the element can cause kidney damage, including fluid loss and disruption of homeostasis. Furthermore, the kidneys' filtration capacity is impaired, and in more extreme cases, it can cause glomerulopathies, osteoporosis, or osteomalacia [4].

Check for updates

Academic Editor: Francesco Bianco

Received: 7 August 2026
Revised: 22 September 2026
Accepted: 1 October 2026
Published: 7 October 2026

Copyright: © 2026 by the authors. Licensee MDPI, Basel, Switzerland. This article is an open access article distributed under the terms and conditions of the Creative Commons Attribution (CC BY) license.

However, there are multiple methods for removing PTEs from water. In this case, bioremediation is a technology that uses biological agents, such as bacteria, yeasts, fungi, and plants, to reduce the effects of the pollutants present in the environment through their transformation or removal [6], and can be carried out directly at the contaminated site. Various methods exist, but the main ones are aerobic biodegradation, anaerobic degradation, phytoremediation, biosorption, and bioaccumulation [7].

In this case, microorganism-mediated bioremediation takes advantage of their ubiquity in the environment, their role in biogeochemical cycles, their metabolic capabilities, and their rapid growth to capture contaminants and thereby prevent their mobilization or, alternatively, reduce their toxicity [8]. The two main types of microorganism-mediated bioremediation are biosorption and bioaccumulation. Biosorption, by itself, is a mechanism that uses biological agents, whether it be organic matter, biomass, or microorganisms, to remove PTEs. It involves a nonspecific physicochemical interaction with adsorbates, generally metal ions, which leads to their binding to cell wall compounds [8,9]. This process is not directly dependent on the organism's metabolic cycle. However, bioaccumulation occurs as a second, metabolically active stage of biosorption. It takes place after a certain period following the initial interaction of the adsorbate with the biosorbent. Ions bound to the cell wall can be translocated into the cell via active transport or carriers [10]. This process results from exposure to water, sediments, or air containing a solute of interest, followed by its absorption, diffusion, and elimination from the organism [11].

Furthermore, the use of lignocellulosic biomass benefits the removal of PTEs, because these types of materials possess a high biosorption capacity associated with the functional groups contained in cellulose, hemicellulose, and lignin, such as hydroxyl, carboxyl, carbonyl, and amine groups [12]. Moreover, the porous structure and cavities of the materials increase the surface area available for adsorption [13]. In this case, rice husks are considered polluting waste due to their excessive presence in agricultural fields and unsuitability for animal feed because of their high silica content, which represents approximately 90% of the ash [14]. Therefore, rice husk reuse is an opportunity to promote a circular economy scheme.

Additionally, using yeasts as biosorbents offers an advantage over bacteria because they produce more biomass and extracellular enzymes. This allows them to adapt more easily to stressful conditions in their environment, including high concentrations of PTEs.

In this regard, biosorption techniques using agro-industrial waste and microbial biomass have been employed as a sustainable alternative due to their low cost, wide availability, and excellent biosorption capacity.

Therefore, this study proposes a sustainable bioremediation strategy by combining lignocellulosic biomass and microorganisms, such as *Rhodotorula* sp., which represent an affordable, non-invasive, and promising option for water quality recovery. This yeast has shown high Cd^{2+} removal efficiencies from water, demonstrating its potential as a biosorbent [15,16]. The main contribution of this study is demonstrating the potential achieved by combining two types of sorbents: one of them is a natural bioproduct (rice husk) and the other a microbial adsorbent (*Rhodotorula* sp.) for the removal of Cd^{2+} from water.

2. Materials and Methods

2.1. Microorganisms and Growth Conditions

The yeast *Rhodotorula* sp. was isolated from the Atenco pier in San Gregorio Atlapulco, Xochimilco. The yeast was inoculated every 4 days to obtain pure colonies. The plates were incubated in a KERN ALT 310-4 incubator (KERN & SohnGmbH, Balingen, Germany) at 28 °C for 48 h, and then stored under refrigeration at 4 °C. The inoculum production

was carried out in a Yeast–Peptone–Dextrose (YPD) medium: polypeptone (20 g/L) (MCD LAB, Tlalnepantla de Baz, Mexico), yeast extract (10 g/L) (MCD LAB, Tlalnepantla de Baz, Mexico), anhydrous D-glucose (20 g/L) (Meyer, Mexico City, Mexico), and, in the case of the solid medium used to maintain the yeast, bacteriological agar (15 g/L) (BD Bioxon, State of Mexico, Mexico) was added.

2.2. Preparation of the Biosorbent (Rice Husk)

The rice husk was washed five times using distilled water to remove contaminants. The husks were then dried at room temperature (25 °C).

2.3. Immobilization of Rhodotorula sp. on Rice Husk

Yeast immobilization was performed using the methodologies of Martini et al. (2010) [17] and Yu et al. (2007) [18], with liquid YPD medium and 5 g of rice husk as fiber. The incubation conditions were repeated for each of the following procedures, incubating at 28 °C with 100 rpm shaking. The media and rice husk were previously sterilized at 121 °C, and aseptic conditions were maintained throughout the methodology. Figure 1 represents the immobilization procedure schematically.

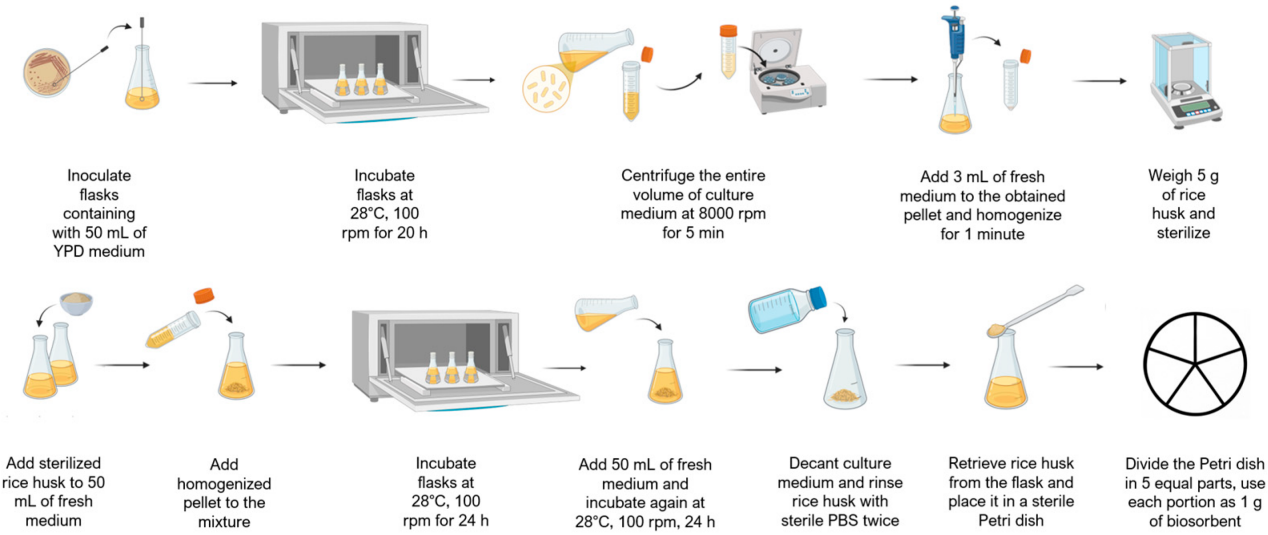


Figure 1. Immobilization technique, modified from Martini et al. (2010) [17] and Yu et al. (2007) [18].

First, a pre-inoculum of yeast was prepared in 125 mL Erlenmeyer flasks containing 50 mL of liquid YPD medium. A single isolated colony was inoculated into the flask containing the fresh medium and incubated for 20 h. The pre-inoculum was then centrifuged at 8000 rpm for 5 min using a Centra-MP4R centrifuge (International Equipment Company, Needham, MA, USA). The resulting cells were resuspended in 50 mL of medium, and 5 g of sterile rice husk was added to the flask containing the inoculum. This was incubated for 24 h under the above-mentioned conditions. After this time, another 50 mL of fresh medium was added to the flask containing the inoculum, and it was incubated again for 24 h. Finally, the liquid medium was decanted, and the rice husk was used for the experiments.

2.4. Scanning Electron Microscopy (SEM) and Evaluation of Rhodotorula sp. Immobilization

Once the above was completed, the microstructure and morphology of the yeast immobilized on the husk were examined using a JEOL-JSM 6510 LV scanning electron microscope (JEOL Ltd., Tokyo, Japan).

Previously, a husk sample was taken and fixed with 2.5% (*v*/*v*) glutaraldehyde in 0.1 M sodium cacodylate buffer, pH 7.2. The sample was then dehydrated with increasing concentrations of ethanol and dehydrated to a critical point with hexamethyldisilazane (Polysciences, Inc., Warrington, PA, USA). The samples were coated with gold using a TED Pella sputtering device (Redding, CA, USA).

To ensure successful immobilization, assays were performed in Petri dishes containing 10 mL of YPD medium. A husk was placed directly in the flask as a positive control, consisting of husk that was in direct contact with the medium, containing *Rhodotorula* sp., without any washing.

For the remaining plates, multiple husks were obtained and placed in sterile 2 mL Eppendorf tubes. The samples were washed in these tubes using 1 mL of sterile phosphate-buffered saline (PBS) (J.T. Baker, Phillipsburg, NJ, USA), mixing for 10 s and carefully removing the liquid. Husks with different washing cycles (1, 2, and 3) were placed on each plate. Each treatment and plate was performed in duplicate. Subsequently, once the above was carried out, the same washing and plating procedure was performed for the negative controls, using the mentioned method except for the pre-inoculum and cell concentration steps. Each plate was incubated for 36 h at 28 °C; afterwards, the yeast growth around the husks was observed.

2.5. Fourier-Transform Infrared Spectroscopy (FTIR)

The functional groups of rice husk samples, both with and without Cd^{2+}, were analyzed using Fourier-transform infrared spectroscopy. Spectral scanning was performed in the 4000–400 cm^{-1} range with a resolution of 2 cm^{-1}, using a Nicolet 6700 spectrometer (Thermo Fisher Scientific, Madison, WI, USA). The data were analyzed based on the signals obtained.

2.6. Batch Adsorption Kinetics

2.6.1. Adsorption Kinetics Using Lignocellulosic Material

Kinetics were performed using untreated rice husk. For this purpose, 250 mL Erlenmeyer flasks containing 200 mL of cadmium solution were used. The solutions were prepared at concentrations of 1, 5, 10, 20, and 25 mg/L using distilled water and cadmium chloride (Meyer, Mexico City, Mexico). The pH was adjusted to 5 and maintained as a controlled experimental condition throughout the adsorption kinetics. Once prepared, 1 g of washed fiber was added, and 10 mL samples of the operating volume were taken during the kinetics, which lasted a total of 8 h. Samples were collected every 30 min for the first 4 h and then every hour thereafter. The flasks were kept under constant agitation at 100 RPM at a temperature of 25 °C. The experiment was performed in duplicate.

2.6.2. Adsorption Kinetics Using Immobilized Yeast

With the conditions described above, the kinetics were performed using the immobilized yeast on the fiber, employing Cd^{2+} solutions with concentrations of 1, 10, and 20 mg/L at pH 5. Using the immobilization procedure described above, the rice husk was recovered and placed in a Petri dish, then distributed evenly throughout the dish, which was divided into 5 equal parts. Each part was considered to be 1 g of dry rice husk, and 1/5 of the divided dish was added to each of the flasks. The samples for this experiment were taken using the same times and volumes as in the kinetics with untreated rice husk.

2.7. Cd^{2+} Quantification

2.7.1. Sample Preparation

Prior to Cd^{2+} quantification, acid digestion was performed on the samples that might have contained biological material. In this context, 9 mL of the samples obtained from the flasks during the kinetics were placed in Teflon tubes, and 1 mL of 68–70% nitric acid

(MEYER) was added. The tubes were then placed in a MarsXpress accelerated reaction microwave digester and treated with one digestion cycle, EPA method 3051-16. Subsequently, the samples were filtered using 8 µm open-pore filter paper.

2.7.2. Determination of Cd^{2+} Concentration

The samples were analyzed using a NexION 350Q ICP-MS plasma spectrometer (PerkinElmer, Waltham, MA, USA). The multi-element standard used to calibrate the ICP-MS instrument and obtain the Cd^{2+} reading was from PerkinElmer (PerkinElmer, Shelton, CT, USA). The detection limit was 0.0001 mg/L for Cd^{2+}. Samples with concentrations greater than 1 mg/L were diluted in a 1:10 ratio with Milli-Q water before analysis.

2.8. Biosorption Equilibrium

Two main parameters were evaluated within the batch adsorption kinetics: the amount of metal adsorbed per gram of adsorbent and the percentage of cadmium ion removal at the end of the process. The first parameter is defined by Equation (1) [19]:

$$q_e = \frac{(C_0 - C_e)V}{m} \quad (1)$$

where

V: Volume of the aqueous phase (solution) [L];

m: Mass of biosorbent used in the assay [mg];

C_0: Initial concentration of Cd^{2+} in the aqueous phase [mg/L];

C_e: Concentration of Cd^{2+} at equilibrium [mg/L];

q_e: Amount of metal adsorbed by the fibers at equilibrium or biosorption capacity [mg/g].

On the other hand, the removal percentage during an adsorption process is shown in Equation (2), according to Tayyab et al. (2025) [20]:

$$\%R = \frac{C_0 - C_e}{C_0} \times 100\% \quad (2)$$

2.9. Adsorption Isotherms

The equilibrium characteristics of adsorption processes can be represented by isotherms. These illustrate the equilibrium relationship between the concentration in the fluid phase and the concentration on the adsorbent particles at a given temperature [21].

2.9.1. Henry Isotherm

This isotherm proposes a linear relationship between the amount adsorbed and the initial adsorbate concentration and states that the adsorption process occurs as a monolayer at low concentrations [13]. This isotherm is represented by Equation (3):

$$q_e = K_p C_e \quad (3)$$

where

K_p: Henry's law partition coefficient [L/g];

C_e: Equilibrium concentration of Cd^{2+} [mg/L].

2.9.2. Langmuir Isotherm

This isotherm proposes that the biosorbent used has a homogeneous surface, adsorption occurs as a monolayer, and the amount of adsorbate does not influence the kinetics. It also assumes that the adsorbed molecules do not interact with each other [13] and

that the adsorption and desorption rates are equal [22]. This isotherm is represented by Equations (4) and (5):

$$\frac{C_e}{q_e} = \frac{1}{q_{max} \cdot K_L} + \frac{1}{q_{max}} \cdot C_e \quad (4)$$

$$R_L = \frac{1}{1 + K_L C_0} \quad (5)$$

where

q_e: Metal adsorbed by the fibers at equilibrium or biosorption capacity [mg/g];
C_e: Cd^{2+} concentration at equilibrium [mg/L];
C_0: Highest initial concentration [mg/L];
K_L: Langmuir constant, related to the binding sites and sorption energy [L/mg];
q_{max}: Maximum biosorption capacity in a monolayer [mg/g].

2.9.3. Freundlich Isotherm

This isotherm assumes that the biosorbent's surface is heterogeneous; therefore, the adsorption process occurs in a multilayer, with interactions between the adsorbed molecules; additionally, the distribution of adsorption energy and surface affinity is not uniform [13,23]. Equation (6) describes this isotherm.

$$\log q_e = \log K_F + \frac{1}{n} \cdot \log C_e \quad (6)$$

where:

K_F: Freundlich constant, related to the adsorption capacity of the adsorbent [L/g];
n: Adsorption intensity [dimensionless];
C_e: Cd^{2+} concentration at equilibrium [mg/L].

2.9.4. Sips Isotherm

This model is considered a combination of the Langmuir and Freundlich models, as it is used to predict adsorption on heterogeneous surfaces. It reduces to the Freundlich model at low pressure and, like the Langmuir model, has a finite saturation limit at high pressure [24]. Therefore, if the adsorbate concentration is low, the model reduces to the Freundlich model, while at high adsorbate concentrations, the Langmuir model is predicted [25]. Equation (7) describes this isotherm.

$$q_e = \frac{q_{max} K_s C_e^n}{1 + K_s C_e^n} \quad (7)$$

where

q_{max}: Maximum adsorption capacity [mg/g];
K_s: Affinity constant of Sips $[mg/L]^{-n}$;
n: Exponent of heterogeneity [Dimensionless].

2.10. Adsorption Kinetics

Kinetics allow us to estimate the adsorption rate using mass transfer coefficients [13].

2.10.1. Pseudo-First Order Kinetics

This type of kinetics indicates physical adsorption, considering that the adsorption rate at binding sites is proportional to the number of unused sites, and assuming that only one ion is adsorbed per binding site. These kinetics are described using Equation (8).

$$ln(q_e - q_t) = ln(q_e - K_1 t) \quad (8)$$

where

q_t: Adsorption capacity at a given time [mg/g];

K_1: Adsorption constant of the pseudo-first-order model [1/h].

2.10.2. Pseudo-Second-Order Kinetics

This model describes the chemical adsorption of the ions, in which electrons are shared between the adsorbent and the metal ions. It considers that the adsorption rate at the binding sites is proportional to the square of the number of unused sites [26]. Equation (9) represents these kinetics.

$$\frac{t}{q_t} = \frac{1}{K_2(q_e)^2} + \frac{t}{q_e} \quad (9)$$

where

q_t: Adsorption capacity at a given time [mg/g];

K_2: Adsorption constant of the pseudo-second order model [g/mgh].

2.11. Statistical Analysis

Different statistical analyses were performed to evaluate the behavior of the obtained responses, comparing the impact of initial concentration, as well as the removal performance (removal percentage, biosorption capacity) of the natural rice husk and the immobilized yeast.

A one-way analysis of variance (ANOVA) was performed individually for each material to identify significant differences between the evaluated concentrations, with a significance level (α) of 0.05. Subsequently, a post hoc test (Tukey, $p < 0.05$) was applied to determine which treatments showed significant differences among themselves and, therefore, were not attributed to random variation. These statistical analyses were performed using OriginPro 8.5.

Isotherms, pseudo-first-order, and pseudo-second-order kinetics were obtained by linear regression using GraphPad Prism 8.0.2, which evaluated the fit of the experimental data to the various models using the coefficient of determination (R^2). In addition, the residual sum of squares and the root mean square error were estimated for the isotherm models to describe in detail their fit to the experimental data.

To compare the responses (removal percentage, biosorption capacity) between the biosorbent materials (untreated rice husk, immobilized yeast), a two-way ANOVA was performed, including a post hoc Tukey test ($p < 0.05$), using GraphPad Prism 8.0.2. The test was performed in order to determine whether the combination of initial concentration and biomaterial used had a significant effect on the evaluated variables.

3. Results and Discussion

3.1. Immobilization of Rhodotorula sp. on Rice Husk Using SEM

Scanning electron microscopy (SEM) micrographs of rice husk after *Rhodotorula* sp. immobilization are shown below.

Figure 2 shows the micrographs of the exterior of the rice husk; these reveal that the fiber has multiple convex protrusions, as seen in Figure 2a–c. Likewise, the residues visible in Figure 2d–f are also commonly found in the fiber, as reported by Sukmana et al. (2025) [27].

On the exterior of the husk, yeast growth is not noticeable. The eruptions on the husk resemble the common structure of untreated fiber without inoculum, as reported by Yefremova et al. (2023) [28]. This may indicate that *Rhodotorula* sp. did not adhere to the outer surface of the husk; however, such conclusions could be evaluated by performing the same immobilization procedure without the inoculum as a negative control. Nevertheless,

on the inner surface of the support, a different morphology can be observed compared to the outer surface, as shown in Figure 3, where oval-shaped bodies can be seen.

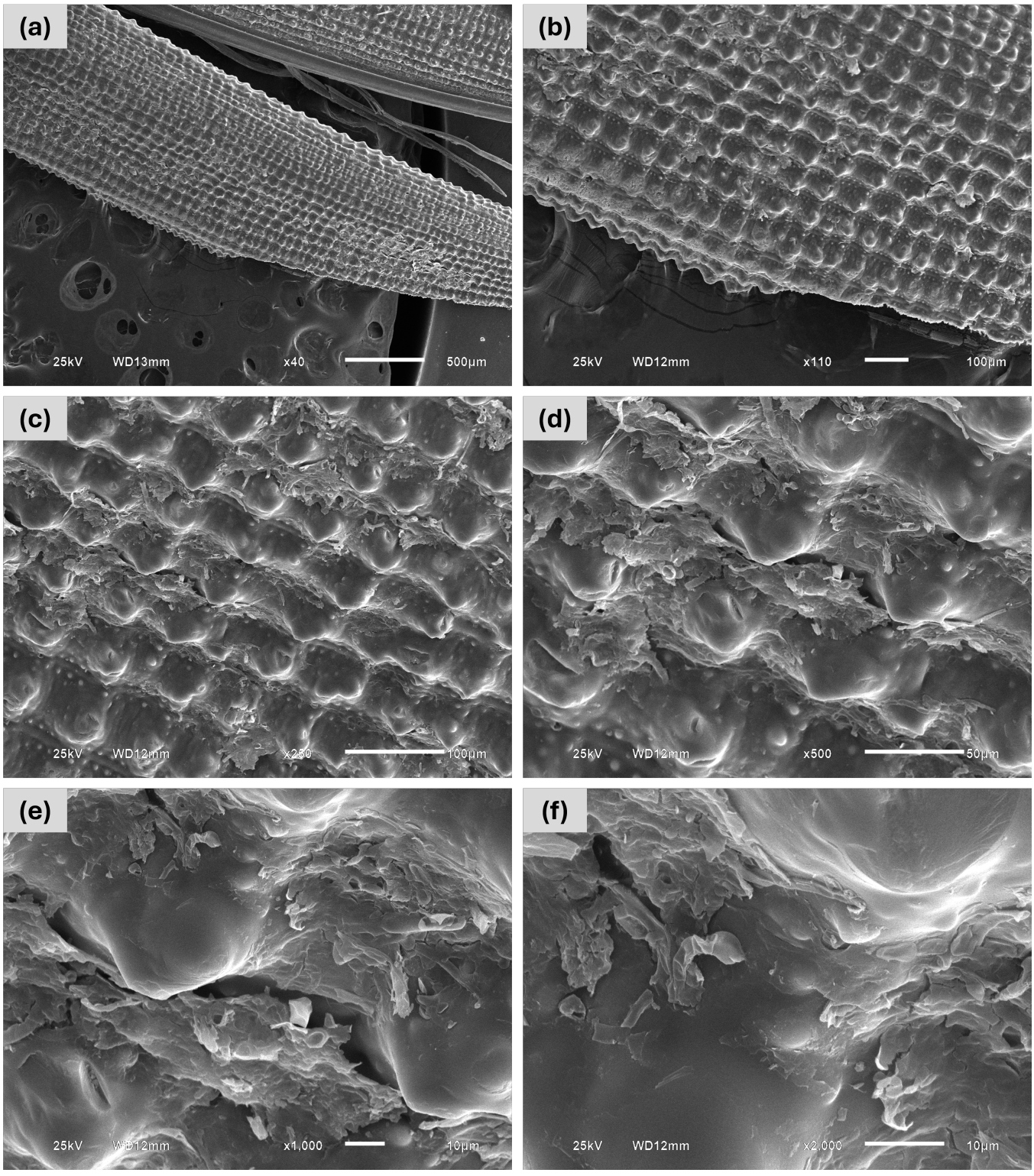


Figure 2. SEM micrographs of the immobilization technique, exterior of the husk, with different magnifications: (**a**) ×40, (**b**) ×110, (**c**) ×250, (**d**) ×500, (**e**) ×1000 and (**f**) ×2000.

In this case, oval bodies similar to those reported by Cha et al. (2014) [29], who immobilized *Saccharomyces cerevisiae* in sawdust to produce ethanol in a continuous column reactor, can be observed in Figure 3e,f. Similarly, in the work of Xue et al. (2025) [30],

these types of bodies, corresponding to *Rhodotorula mucilaginosa* immobilized in polyvinyl alcohol fiber, are also observed.

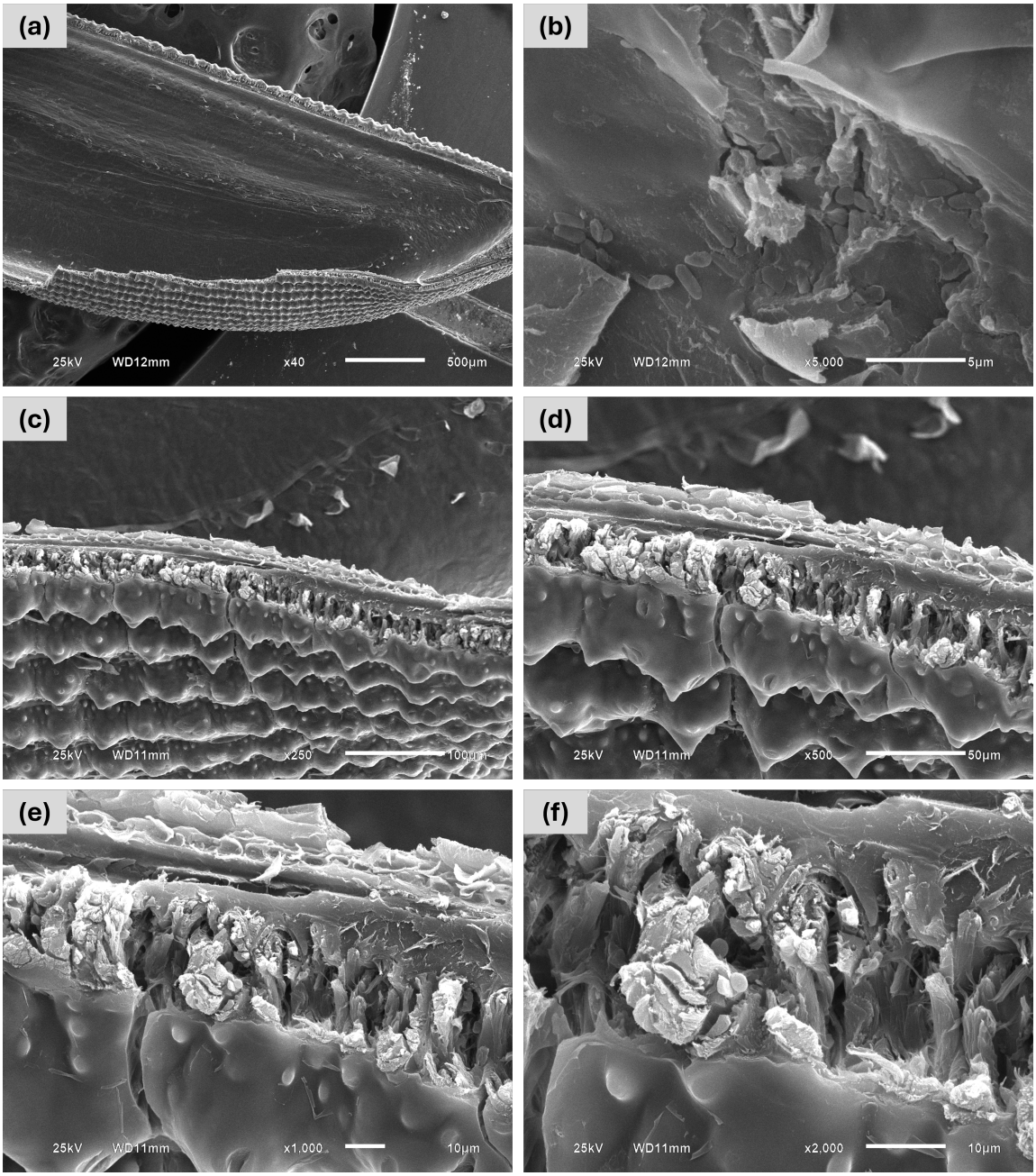


Figure 3. SEM micrographs of the immobilization technique, interior of the husk, with different magnifications: (**a**) ×40, (**b**) ×5500, (**c**) ×250, (**d**) ×500, (**e**) ×1000 and (**f**) ×2000.

Furthermore, to verify whether the yeast was truly immobilized in the biosorbent, immobilization assays were performed. Figure 4a, at the top, shows the positive control, which corresponds to one of the rice husks without PBS wash. Conversely, the negative controls, shown at the bottom, correspond to the husk incubated in culture medium without inoculum and subjected to 1, 2, and 3 PBS washes. Figure 4b shows the plates with the yeast immobilized in the biosorbent after the different PBS washes, where it is visible that the yeast was indeed immobilized on the rice husk. The yeast growth can be observed as a salmon color around the husk, which is characteristic of *Rhodotorula* spp. due to its carotenoid production [31].

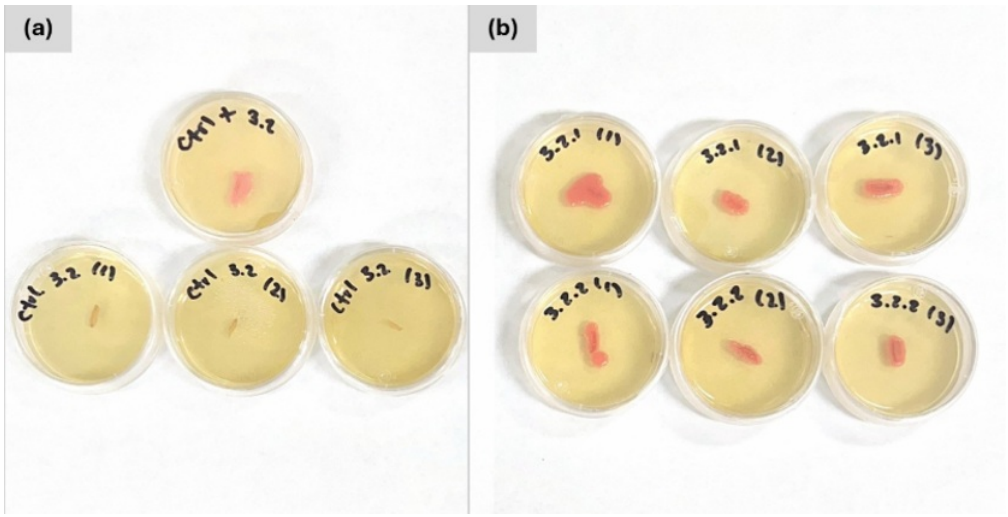


Figure 4. Assays performed for the immobilization of *Rhodotorula* sp. (**a**) Positive (**top**) and negative (**bottom**) controls with 1, 2, and 3 PBS washes; (**b**) assays with 1, 2, and 3 PBS washes, duplicate.

3.2. Fourier-Transform Infrared Spectroscopy (FTIR) of Rice Husk

Fourier-transform infrared (FTIR) spectroscopy was used to identify the main functional groups present in the rice husk samples before Cd^{2+} adsorption (Figure 5a) and after Cd^{2+} adsorption (Figure 5b).

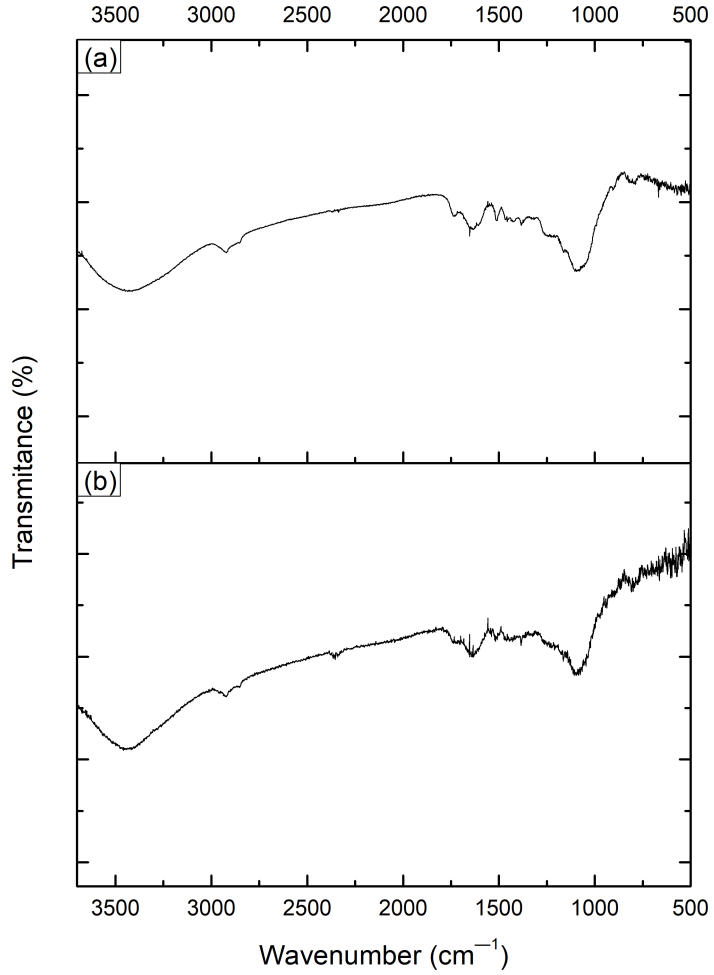


Figure 5. Fourier-transform infrared (FTIR) spectra of (**a**) rice husk without Cd^{2+} and (**b**) rice husk after Cd^{2+} adsorption.

The main absorption bands were observed in the 3448.29–3320 cm^{-1} region, corresponding to O–H stretching vibrations associated with alcoholic/hydroxyl and phenolic hydroxyl groups, and at approximately 2920 cm^{-1}, corresponding to C–H stretching vibrations of CH_2 groups. Additionally, bands around 1730 and 1630 cm^{-1} were assigned to C=O and C=C stretching vibrations, respectively, associated with carbonyl-containing structures and aromatic compounds. Bands around 1430 cm^{-1} were attributed to O–H and C–O vibrations, particularly those associated with phenolic structures. The bands at approximately 1084 and 786 cm^{-1} were assigned to Si–O–Si stretching and bending vibrations, respectively. Meanwhile, the band around 1030 cm^{-1} was associated with C–O and C–C–O vibrations, which are characteristic of lignocellulosic components such as cellulose, hemicellulose, and lignin.

Following Cd^{2+} adsorption, changes in the position and intensity of characteristic bands were observed, particularly in the regions associated with O–H, C=O, and C=C groups. These spectral changes may indicate the involvement of these functional groups in Cd^{2+} binding to the rice husk [32–34].

3.3. Batch Adsorption Kinetics Studies

3.3.1. Adsorption Kinetics Using Rice Husk

The results of the batch adsorption kinetics for rice husk are presented below. This process was characterized by the continuous contact of the adsorbent with the treated solution; for this reason, the concentration of Cd^{2+} ions in the solution decreases over time as the adsorbent's binding sites are used by this element.

Figure 6 describes the batch adsorption kinetics performed at different initial concentrations, using only rice husk as the adsorbent. To compare the behavior of the five experiments performed, the concentrations measured over time were divided by the initial concentration to obtain values from 0 to one and construct the breakthrough curves. This is done to identify breakthroughs and saturation times [35].

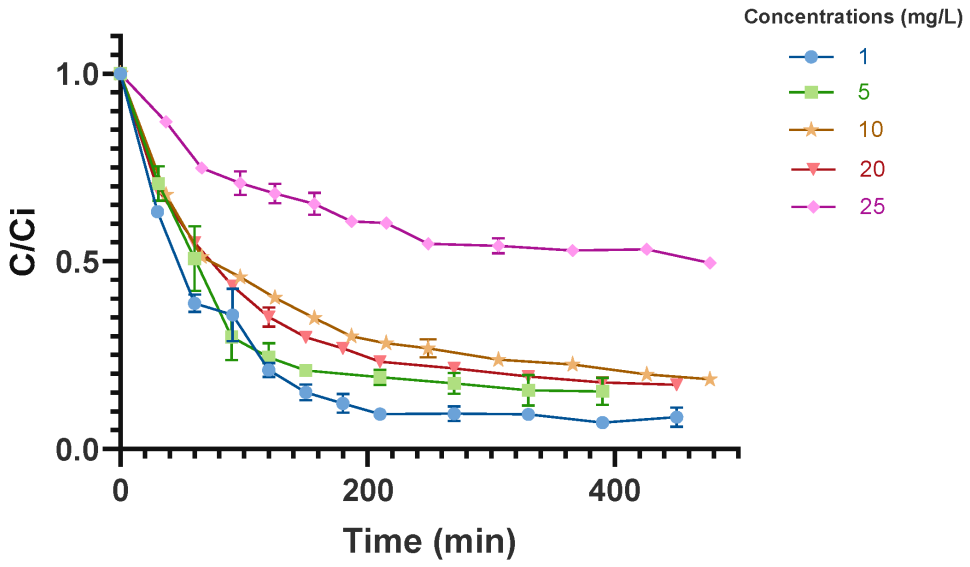


Figure 6. Batch adsorption kinetics of rice husk.

In this case, the curves exhibited the behavior of typical adsorption saturation curves, in which the Cd^{2+} concentration in the solution decreased after the addition of the biosorbent and progressively approached a stable value. The equilibrium time was determined from the kinetic profiles by identifying the point at which no appreciable changes in the Cd^{2+} concentration (C_t/C_i) were observed with further increases in contact time. Based on

this criterion, the equilibrium times were 210, 330, 426, 390, and 366 min for initial Cd^{2+} concentrations of 1, 5, 10, 20, and 25 mg/L, respectively. The subsequent measurements were used to confirm the stabilization of the systems after these times. The equilibrium concentrations (C_e) obtained at these times were subsequently used to calculate the equilibrium adsorption capacity (q_e).

Moreover, a difference can be observed in the ratio between the measured and initial Cd^{2+} concentrations (C_t/C_i) at an initial concentration of 25 mg/L. At this concentration, the curve remained below 0.5, whereas the curves corresponding to the other initial concentrations remained above 0.7. This behavior indicates a greater relative decrease in the aqueous Cd^{2+} concentration at 25 mg/L. This difference may be associated with the relationship between the initial Cd^{2+} concentration and the availability of adsorption sites, as well as with the adsorption capacity of the biosorbent.

In this context, several studies have reported different equilibrium times depending on the experimental conditions. For example, Montalvo-Andía et al. (2022) [36] used rice husk to remove 10 mg/L of Cd^{2+} and reported that equilibrium was reached after 8 h using 150 mg of biosorbent. In another study, Nemah and Naife (2024) [37] used the same biosorbent (2.5 g) to remove 100 mg/L of Cd^{2+}, reaching equilibrium after 160 min. These studies, together with the present results, indicate that the time required to reach equilibrium depends on the operating conditions, particularly the initial metal concentration and the amount of biosorbent used. Furthermore, the rapid decrease in Cd^{2+} concentration during the initial stages of the process can be attributed to the availability of binding sites, which progressively become occupied as adsorption proceeds, eventually reaching a state in which the adsorption and desorption rates become approximately constant [22].

The solution pH is a key parameter affecting Cd^{2+} adsorption, as it influences the protonation state of functional groups on the biosorbent surface and the behavior of Cd^{2+} in aqueous solution. At low pH, the protonation of functional groups can increase competition between H^+ and Cd^{2+} ions for available adsorption sites, potentially limiting Cd^{2+} adsorption [38]. As pH rises, the deprotonation of these groups can facilitate the interaction between Cd^{2+} and the biosorbent surface [39]. However, at higher pH values, Cd^{2+} hydrolysis and precipitation may occur [40], making it difficult to distinguish whether the mechanism responsible for Cd removal is adsorption or precipitation.

On the other hand, Figure 7 corresponds to the removal percentages and the adsorption capacity of the kinetics carried out.

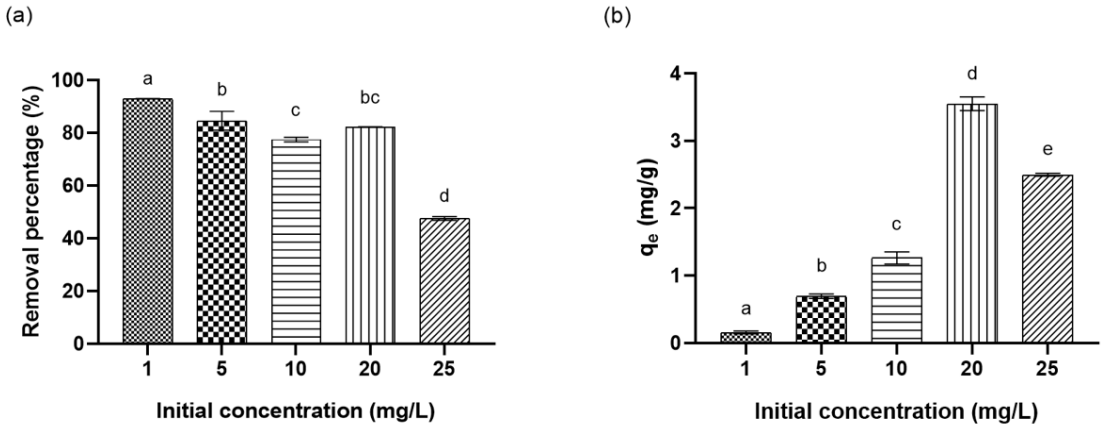


Figure 7. Differences between different initial concentrations in the adsorption kinetics with natural rice husk (untreated): (**a**) removal percentage of Cd^{2+} and (**b**) biosorption capacity of Cd^{2+}. The letters show statistically significant differences ($p < 0.05$) between the concentrations used.

In the case of Figure 7a, for each of the evaluated Cd^{2+} concentrations (1, 5, 10, 20, and 25 mg/L), the removal percentages were 92.99%, 84.63%, 77.48%, 82.27%, and 47.58%, respectively. In addition, higher removal percentages were observed using lower initial concentrations. Within the concentration range of 5 to 20 mg/L, no statistically significant differences were observed ($p < 0.05$); however, at concentrations of 1 and 25 mg/L of Cd^{2+}, significant differences were observed, with the lower concentration exhibiting the highest removal percentage. In this regard, increasing the initial concentration leads to a greater number of binding sites being occupied until the saturation point is reached and the ions remain in solution, as occurs with the 25 mg/L concentration. Therefore, at lower concentrations, higher removal percentages are obtained due to the availability of binding sites and less competition between ions [36].

In turn, studies such as that of Montalvo-Andía et al. (2022) [36] mention that removal percentage decreases at higher concentrations; using 150 mg of rice husk, removal percentages of 62%, 53%, and 29% were obtained at initial concentrations of 9.52, 19.48, and 48.56 mg/L of Cd^{2+}, respectively. In the work carried out by Tayyab et al. (2025) [20], a decrease in Cd^{2+} removal was observed as the initial concentration of the solution increased, using solutions of 200–800 mg/L with 0.5 g of the biosorbent.

In the case of Figure 7b, the biosorption capacity (mg/g) for each of the kinetics performed with rice husk at Cd^{2+} concentrations (1, 5, 10, 20, and 25 mg/L) was 0.155, 0.695, 1.262, 3.538, and 2.495, respectively; therefore, statistically significant differences ($p < 0.05$) were observed when using different initial concentrations of Cd^{2+}. The q_e with the highest value corresponds to the C_i of 20 mg/L, which is consistent with greater availability of ions as the concentration increases. Likewise, although at 25 mg/L the availability of ions is also high, the saturation of the adsorbent leads to a lower biosorption capacity. This is due to the depletion of potential binding sites during the process [32]. Additionally, determining the capacity of the adsorbent is necessary to select the appropriate material for the process, as well as to improve its biosorption capacity through chemical or physical methods [41].

3.3.2. Adsorption Kinetics Using Immobilized *Rhodotorula* sp.

Rhodotorula sp. was immobilized on rice husk to exploit the microorganism's capabilities to assimilate metal ions, as well as the previously described properties of rice husk as an adsorbent. The synthesis of a new biosorbent such as the one presented here requires an individual analysis to define the main mechanisms involved in the adsorption process.

Figure 8 shows the adsorption kinetics of the material at 1, 10, and 20 mg/L concentrations. Different concentrations were used, in comparison with the untreated rice husk, because the statistical results did not show significant differences between the other omitted treatments. The kinetics follow a typical batch break curve pattern, and as the initial concentration increases, the equilibrium concentration is reached over a longer period. In turn, the saturation of the adsorbent increases relative to the initial concentration, since lower ratios of measured to initial concentration are obtained. Furthermore, equilibrium is reached at 157, 247, and 307 min for 1 mg/L, 10 mg/L, and 20 mg/L, respectively.

Figure 9a shows the cadmium removal percentages obtained in the kinetics with immobilized yeast. The percentages obtained for concentrations of 1, 10, and 20 mg/L were 99.79%, 95.43%, and 82.54%, respectively. The removal percentage again decreases as the initial Cd^{2+} concentration increases. However, no statistically significant differences were found between initial concentrations, which differs from the results obtained with the untreated rice husk. This may indicate that the yeast enhances removal, even at higher concentrations, and reduces the statistically significant differences.

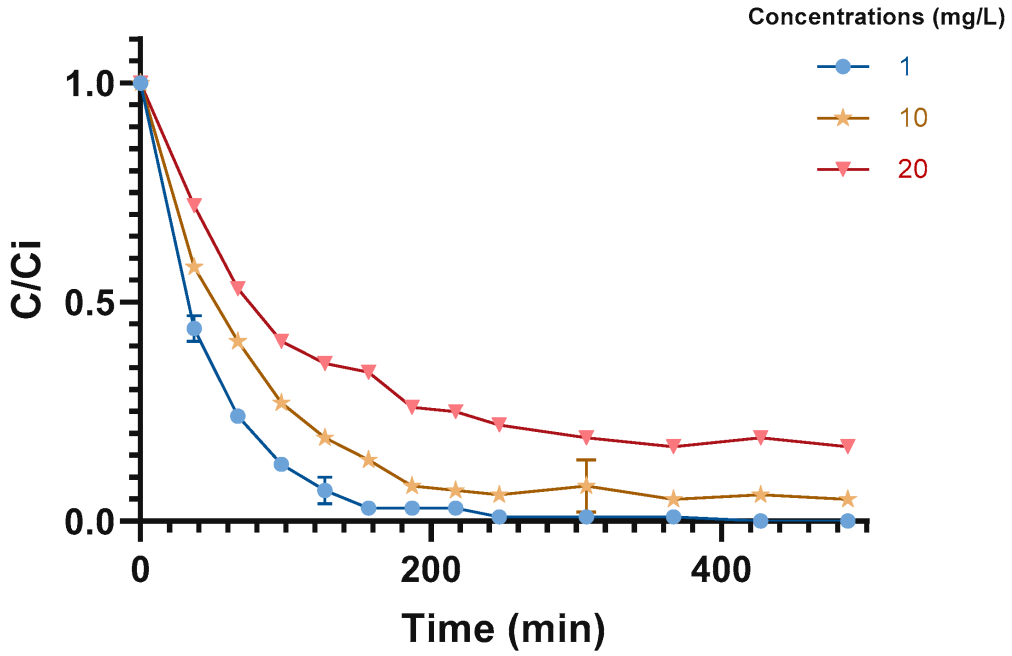


Figure 8. Batch adsorption kinetics of immobilized yeast.

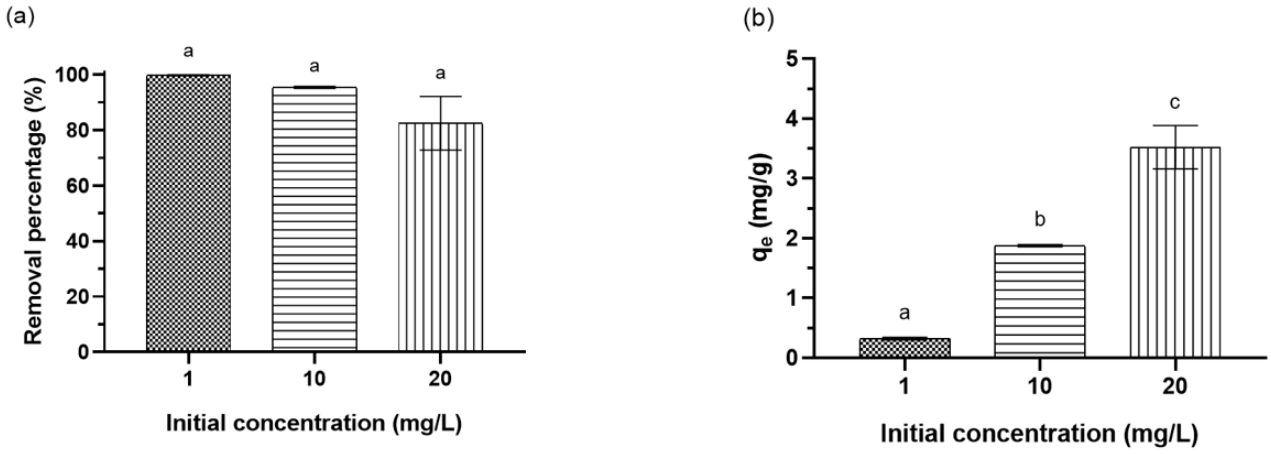


Figure 9. Differences between different initial concentrations in the adsorption kinetics using immobilized *Rhodotorula* sp.: (**a**) removal percentage of Cd^{2+} and (**b**) biosorption capacity of Cd^{2+}. The letters show statistically significant differences ($p < 0.05$) between the concentrations used.

In this context, other studies have been conducted using microorganisms and materials derived from lignocellulosic biomass. In the study by Koippully & Nair et al. (2023) [42], biochar derived from rice husk and *Pseudomonas stutzeri* were used. With this combination, removal percentages of approximately 95% were obtained, starting with an initial concentration of 10 mg/L. These removal percentages were higher compared to the fiber alone and the free microorganism. In another study by Medina-Acevedo (2020) [43], in which a bacterial consortium was immobilized on *Agave angustifolia* to remove cadmium, with an initial concentration of 100 mg/L, the highest removal percentage was 29.95%, lower than the results reported with the untreated fiber (71.33%). This may indicate that the removal effectiveness of the biosorbent combination depends on the microorganism and the chosen support, since certain systems do not offer a synergistic benefit.

Figure 9b shows the biosorption capacity of the material at different concentrations. Biosorption capacities of 0.323, 1.877, and 3.523 mg/g were obtained using concentrations of 1, 10, and 20 mg/L.

In this case, as with the untreated rice husk, the biosorption capacity of the material increases as the initial cadmium concentration increases, and the difference between concentrations is statistically significant. This is consistent with the increased availability of ions that can be adsorbed while working with the same amount of adsorbent. The adsorption capacities obtained at 1 and 10 mg/L for the biosorbent with immobilized yeast are higher compared to the procedures performed using only rice husk.

Furthermore, it is important to distinguish between biosorption and bioaccumulation when evaluating Cd^{2+} removal by microorganisms. Accordingly, in the present study, the term Cd^{2+} removal was used in terms of the decrease in Cd^{2+} concentration in the aqueous phase and the corresponding adsorption capacity. However, specific biomass desorption and digestion experiments were not performed; therefore, it was not possible to experimentally distinguish the contribution of surface biosorption from intracellular bioaccumulation.

Regarding this response, a study by Ali et al. (2021) [44], which used a biosorbent consisting of *Penicillium chrysogenum* and *Cephalotheca foveolata* immobilized on loofah to remove Cd^{2+} from water, found that a higher initial concentration of the element increased the biosorbent's capacity. The results of combining the fiber and microorganisms showed a greater adsorption capacity compared to untreated fiber and free cells.

3.4. Adsorption Isotherms Modeling

3.4.1. Isotherms Using Rice Husk

Table 1 presents the results obtained for fitting the kinetics to the Henry, Langmuir, Freundlich, and Sips isotherms. The minimum fit to the Henry isotherm indicates that there is a linear relationship between the amount of adsorbent and adsorbate [22]. The best fit was obtained for the Sips isotherm with an R^2 = 0.9970, followed by the Langmuir model with an R^2 = 0.9540.

Table 1. Parameters obtained from fitting the isotherms using rice husk as a biosorbent.

Model	Parameters	SSRes	RMSE	R^2
Langmuir	K_L (L/mg) = 0.9345 q_{max} (mg/g) = 2.7582	2.1860	0.6612	0.9540
Freundlich	K_F (L/g) = 0.9232 1/n = 0.5993	5.1318	1.0131	0.8928
Henry	K_p (L/g) = 0.1622	10.4478	1.4455	0.3399
Sips	q_{max} (mg/g) = 7.7378 n = 1.3409 Ks $((mg/L)^{-n})$ = 0.1485	0.0609	0.1424	0.9977

The best fit to the Sips isotherm could be due to the combination of advantages of the Langmuir and Freundlich systems. The parameters obtained using this isotherm showed a qmax of 7.7378 (mg/g), n = 1.3409, and Ks = 0.1485 $(mg/L)^{-n}$; this suggests that the process does not strictly follow the ideal conditions assumed by the Langmuir model and that the Sips model provides a more adequate representation of the adsorbent-adsorbate system characteristics.

These results are comparable to those presented by Wei et al. (2026) [45], where they evaluated Cd^{2+} removal using rice husk biochar, and the study by Et-Tanteny et al. (2025) [46], for Cd^{2+} removal using a clay-chitosan composite. In the case of Nemah and Naife (2024) [37], the results were the opposite, as they better fit the Freundlich isotherm, while Montalvo-Andía et al. (2022) [36], who used untreated rice husk, better fit the Langmuir isotherm.

3.4.2. Isotherms Using Immobilized *Rhodotorula* sp.

Regarding the equilibrium behavior of the system with immobilized *Rhodotorula* sp., the best fit was obtained with the Sips isotherm (R^2 = 0.9989). This suggests a hybrid mechanism that incorporates both monolayer adsorption and surface heterogeneity [45]. Table 2 shows the isotherms and the parameters obtained from them.

Table 2. Parameters obtained from the isotherm fittings using immobilized *Rhodotorula* sp.

Model	Parameters	SSRes	RMSE	R^2
Langmuir	K_L (L/mg) = 17.8764 q_{max} (mg/g) = 3.3078	1.3098	0.5118	0.9918
Freundlich	K_F (L/g) = 2.1928 1/n = 0.1993	6.2738	1.1201	0.6042
Henry	K_p (L/g) = 0.0534	23.1491	2.1517	0.3174
Sips	q_{max} (mg/g) = 3.3607 n = 0.9475 Ks $((mg/L)^{-n})$ = 41.4835	0.0069	0.0480	0.9989

Regarding the parameters related to the isotherm, the parameter value n was 0.9475, close to unity, while the Sips constant (K_s) had a value of 41.4835 $(mg/L)^{-n}$, in addition to an SSRes of 0.0069 and an RMSE of 0.0480 mg/g. However, although the Langmuir model showed a high fit (R^2 = 0.9918), the considerably lower SSRes and RMSE values obtained using the Sips model indicate a better representation of the experimental data.

The Sips isotherm provided a better fit than the Langmuir model, which may be associated with the heterogeneous nature of the adsorption sites present in the biosorbent (*Rhodotorula* sp.). Unlike the Langmuir model, which assumes a homogeneous surface with equivalent adsorption sites [25], the Sips model can account for adsorption systems containing sites with different affinities, because it predicts adsorption on heterogeneous surfaces [25,45]. In the present system, the immobilized yeast may contain different functional groups capable of interacting with Cd^{2+} through distinct mechanisms, which could explain the improved fit obtained with the Sips model.

In this context, there are several studies on the removal of Cd^{2+} using various microorganisms. One of them was the work carried out by Quintelas et al. (2009) [47], in which Cd was removed using *Escherichia coli* on zeolite NaY, in which the best fit was obtained with the Sips isotherm (R^2 = 0.89). Likewise, the study carried out by Shen et al. (2017) [48] shows that an immobilized microalgae (*Chlorella* sp.)–biochar complex also fits the Sips model best, with an R^2 = 0.95, q_{max} = 186.03, and K_s = 0.03. However, there are other studies, such as that of Hegazy et al. (2023) [49], in which inactivated archaeal biomass was used for the removal of Cd^{2+}. In this case, the best fit was obtained for Langmuir with an R^2 = 0.9072, and q_{max} = 128.21 mg/g was obtained. Another study using microalgae (*Chlorella vulgaris*, *Coelas-trella* sp. and *Scenedesmus obliquus*) was carried out by Plöhn et al. (2021) [50], where the results were better fitted to the Langmuir isotherm compared to that of Freundlich.

3.5. Adsorption Kinetics Modeling

3.5.1. Adsorption Kinetics Modeling Using Rice Husk

Adsorption kinetics allow us to establish the rate-limiting steps of the adsorption process, making it possible to calculate the adsorption rate and determine the performance of an adsorbent [51]. Table 3 details the parameters obtained for the pseudo-first-order and pseudo-second-order adsorption kinetics.

Table 3. Parameters obtained from the pseudo-first- and pseudo-second-order kinetics, using rice husk.

Adsorption Kinetics	Parameter	Initial Concentration (mg/L)				
		1	5	10	20	25
Pseudo-first-order	q_e (mg/g)	0.1369	0.6641	1.1387	3.3089	2.0854
	K_1 (1/h)	0.0161	0.0161	0.0110	0.0116	0.0062
	R^2	0.9298	0.9607	0.9942	0.9869	0.9586
Pseudo-second-order	q_e (mg/g)	0.1741	0.8001	1.5004	4.0619	2.9372
	K_2 (g/mgh)	0.1444	0.0259	0.0100	0.0042	0.0028
	R^2	0.9951	0.9892	0.9966	0.9985	0.9826

Fittings were made for each of the initial concentrations evaluated. In all cases, the best fit was obtained for the pseudo-second-order kinetics, particularly at a concentration of 10 mg/L with an R^2 of 0.9966.

These results match those of Nemah & Naife (2024) [37], where the data best fit the pseudo-second-order kinetics (0.9984), using untreated rice husk at a Cd^{2+} concentration of 100 mg/L. When compared with other lignocellulosic biosorbents such as sugarcane bagasse, in the study by Din et al. (2024) [19], the fit obtained was 0.998 for pseudo-second-order kinetics, with concentrations of 5 to 25 mg/L.

Therefore, the results suggest that a better fit to pseudo-second-order kinetics indicates that the main adsorption mechanism of the biosorbent is chemisorption, and that the system depends on the characteristics of the adsorbent and the molecules in solution [27]. This means that the bonding of the adsorbate to the binding site is stronger than in physical adsorption. The type of phenomenon governing the adsorption process is important because it determines whether the adsorbent is reusable through a desorption procedure. In addition, a better fit to pseudo-second-order kinetics can elucidate the reversibility of the process, as well as its effectiveness in removal without desorption processes occurring, especially over time [13,36].

3.5.2. Adsorption Kinetics Modeling Using Immobilized *Rhodotorula* sp.

Table 4 summarizes the main parameters of the pseudo-first-order and pseudo-second-order kinetics of the immobilized *Rhodotorula* sp. For each of the initial concentrations evaluated, the best fit was obtained for the pseudo-second-order models, indicating that the process occurs due to a chemisorption phenomenon [52]. The best fit was obtained for 1 mg/L (0.9986); however, all concentrations exceeded an R^2 value of 0.9944.

Table 4. Parameters obtained from the pseudo-first- and pseudo-second-order kinetics, using immobilized *Rhodotorula* sp.

Adsorption Kinetics	Parameter	Initial Concentration (mg/L)		
		1	10	20
Pseudo-first-order	q_e (mg/g)	0.1417	1.2122	3.9496
	K_1 (1/h)	0.0133	0.0119	0.0130
	R^2	0.9174	0.8359	0.9687
Pseudo-second-order	q_e (mg/g)	0.3391	2.0648	4.0938
	K_2 (g/mgh)	0.1470	0.0120	0.0037
	R^2	0.9986	0.9952	0.9944

The microorganism, in addition to contributing to physical adsorption onto its cell wall, removes Cd^{2+} ions through processes dependent on its metabolism; thus, the process

is not only physical. Furthermore, the results match a Langmuir R_L close to zero, indicating an irreversible process, characteristic of some chemisorption processes [22].

Considering that the experiments performed do not differentiate which ions are internalized by the yeast and which have been adsorbed by the combined material, it is appropriate to consider that the process occurs as pseudo-second-order kinetics. These results agree with the study carried out by Hegazy et al. (2023) [49] using inactivated archaeal biomass, where the best fit was obtained for pseudo-second-order kinetics, with an R^2 of 0.9965 compared to 0.1646 for pseudo-first-order kinetics.

3.6. Comparison of Biosorbent Performance

Figure 10 displays the adsorption kinetics executed with the same amount of rice husk and immobilized yeast. Compared to the results using the untreated husk, the new material saturates less than the fiber at 1 and 10 mg/L. The addition of yeast causes the process to reach equilibrium in a shorter time. At 20 mg/L, the behavior of both materials is similar; thus, it can be inferred that the joint use of yeast and rice husk is beneficial at concentrations below 20 mg/L.

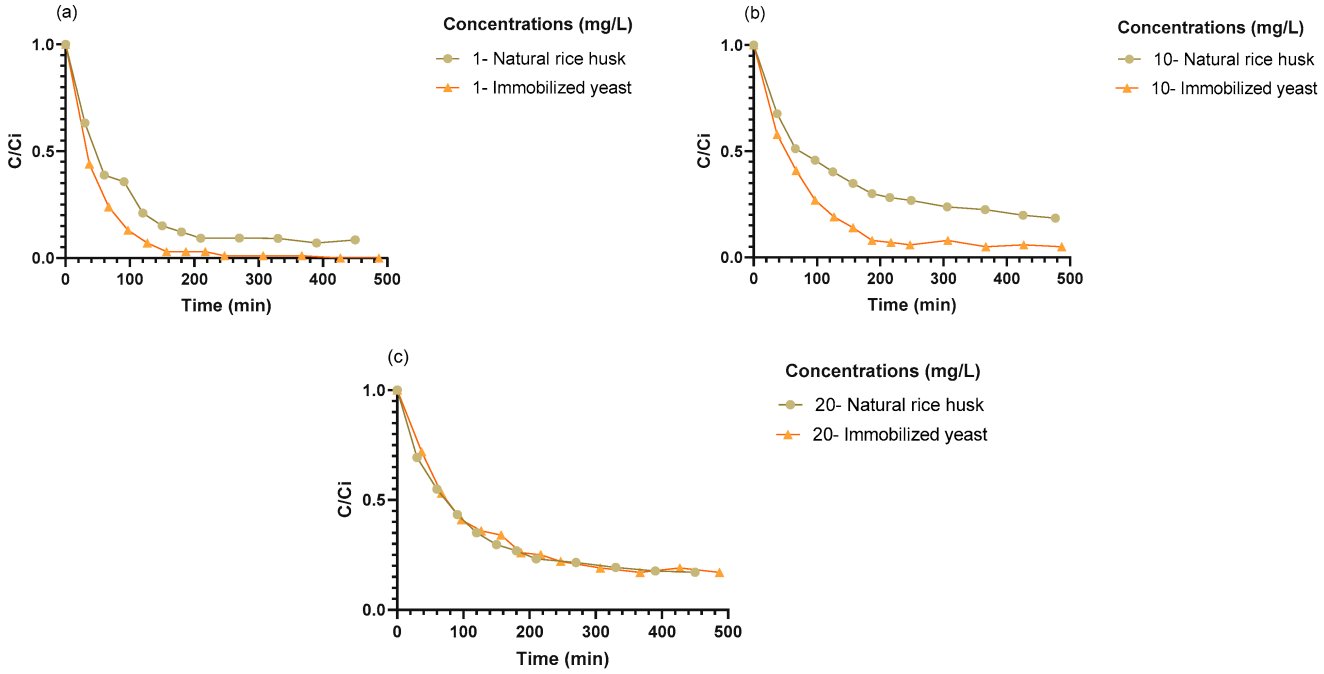


Figure 10. Adsorption curves of the kinetics performed with rice husk and immobilized yeast in the batch system. Initial Cd concentration: (**a**) 1 mg/L, (**b**) 10 mg/L, (**c**) 20 mg/L.

Figure 11a represents the removal percentages obtained in each of the treatments, while Figure 11b shows the biosorption capacity. In general, yeast showed greater Cd^{2+} removal at concentrations of 1 and 10 mg/L; statistically significant differences were observed between the use of husk and yeast immobilized at 10 mg/L ($p < 0.05$), while there were no statistical differences between the other initial concentrations used. It should be noted that, in all the assays carried out with yeast, higher or equal removal percentages were obtained against natural rice husk.

Regarding biosorption capacity, statistically significant differences were observed among the initial concentrations, with an increase in biosorption capacity as the initial concentration increased. However, there are no statistically significant differences between untreated husk and the immobilized yeast ($p < 0.05$). These results indicate that immobilized yeast does not increase the number of ions adsorbed per gram of adsorbent. This

might be explained by two main factors: first, the difference in mass associated with yeast growth throughout the process was not estimated; and, within the immobilization process, the microorganism itself occupies some of the available binding sites of the husk [53,54]. However, the biosorption capacity of the material may benefit from the yeast's own metabolically active mechanisms for PTE removal, as well as from the physical adsorption associated with the cell wall of the microorganism [9,55,56]. Therefore, the yeast does not exert a statistically significant positive or negative effect on the overall biosorption capacity of the novel biosorbent.

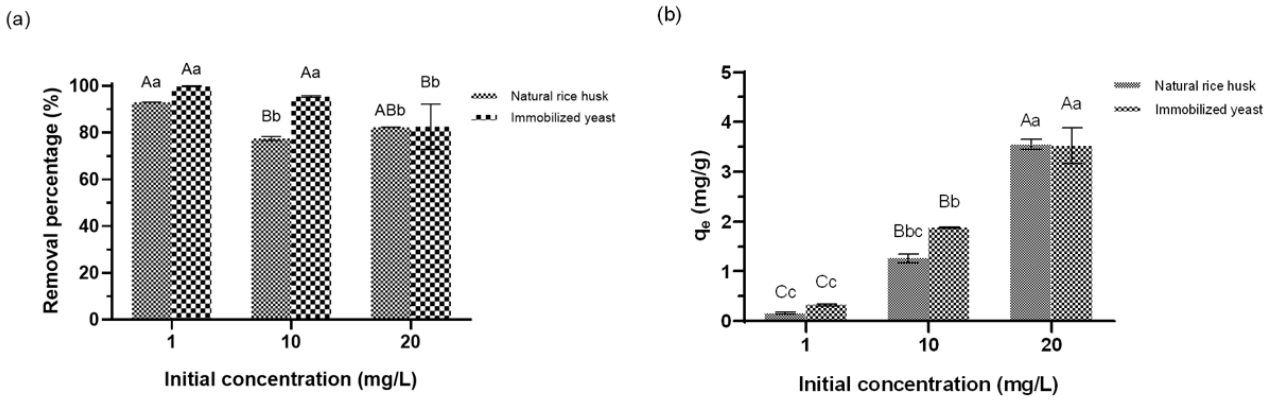


Figure 11. Differences between different initial concentrations in the adsorption kinetics using rice husk and immobilized yeast: (**a**) removal percentage of Cd^{2+} and (**b**) biosorption capacity of Cd^{2+}. Uppercase letters show statistically significant differences ($p < 0.05$) between the concentrations used in the same treatment. Lowercase letters indicate statistically significant differences ($p < 0.05$) at the same concentration using different treatments.

4. Conclusions

Rice husks proved to be a promising, low-cost biosorbent for the removal of Cd^{2+} from water, acting simultaneously as an adsorbent material and as a support for the immobilization of *Rhodotorula* sp., thus promoting the utilization of an agro-industrial waste for which few applications have been documented. Furthermore, micrographs reveal yeast growth within the internal cavities of the lignocellulosic fiber, demonstrating that this type of microorganism can be successfully immobilized on rice husk, thereby adding value to the waste product. The kinetic studies and adsorption isotherms indicated that the removal of Cd^{2+} was best fitted to the pseudo-second-order model, which suggests the possible involvement of interactions between Cd^{2+} and the active sites of the adsorbent, and to the Sips isotherm model, which proposes an adsorption behavior associated with a heterogeneous surface and sites with different affinities for Cd^{2+}. Immobilizing *Rhodotorula* sp. on this material increased removal efficiency from 92.99% (only with rice husk) to 99.79% at an initial concentration of 1 mg/L, without causing significant changes in biosorption capacity. These results suggest that incorporating the yeast can enhance Cd^{2+} removal efficiency under the tested conditions, although its contribution to the material's total capacity may be limited by the amount of immobilized biomass. Overall, immobilizing yeast on rice husk represents a promising strategy for developing biosorbent materials from agro-industrial waste, offering a potentially sustainable and low-cost alternative. However, future studies should evaluate different biomass loadings to determine their influence on biosorption capacity and determine the microorganism's specific contribution to the removal process.

Author Contributions: Conceptualization, methodology: S.M.R.-S. and A.K.I.F.-T.; investigation, validation, visualization, writing—original draft preparation, writing—review and editing: S.M.R.-S., A.K.I.F.-T., and R.R.-V.; formal analysis: S.M.R.-S. and A.K.I.F.-T.; funding acquisition, project administration, Supervision: R.R.-V. All authors have read and agreed to the published version of the manuscript.

Funding: This work was supported by the Secretaría de Ciencia, Humanidades, Tecnología e Innovación (SECIHTI) with a SNII research assistantship awarded to Ramírez-Sologuren S.M. (No. 2178238) and a postdoctoral scholarship awarded to Flores-Trujillo A.K.I. (No. 592589).

Data Availability Statement: The original contributions presented in this study are included in the article. Further inquiries can be directed to the corresponding authors.

Acknowledgments: The authors are grateful to Daniel Talámas-Lara, a member of the Electron Microscopy Unit of the National Experimental Services Laboratories (LaNSE) at CINVESTAV, for his support in sample preparation and micrograph acquisition with the TEM equipment. They also acknowledge Fannis Missirlis of the Department of Physiology of CINVESTAV for his collaboration in the analysis of the samples by ICP-OES. Furthermore, the authors are grateful for the technical support provided by Marcela Guerrero, from the Physics Department of CINVESTAV, for her support in the FTIR analysis.

Conflicts of Interest: The authors declare no conflicts of interest.

Abbreviations

Cd	Cadmium
PTE	Potentially toxic element
K_P	Henry's law partition coefficient
C_e	Equilibrium concentration
q_e	Metal adsorbed by the fibers at equilibrium or biosorption capacity
C_0	Highest initial concentration
K_L	Langmuir constant
q_{max}	Maximum biosorption capacity in a monolayer
K_F	Freundlich constant
n	Adsorption intensity
K_s	Affinity constant of Sips
q_t	Adsorption capacity at a given time
K_1	Adsorption constant of the pseudo-first-order model
K_2	Adsorption constant of the pseudo-second-order model
ANOVA	Analysis of variance
SEM	Scanning electron microscopy
C_i	Initial concentration
SSRes	Sum of squares of the residues
RMSE	Root mean square error

References

1. Musie, W.; Gonfa, G. Fresh water resource, scarcity, water salinity challenges and possible remedies: A review. *Heliyon* **2023**, *9*, e18685. [CrossRef]
2. Nieder, R.; Benbi, D.K. Potentially toxic elements in the environment—A review of sources, sinks, pathways and mitigation measures. *Rev. Environ. Health* **2024**, *39*, 561–575. [CrossRef]
3. De Almeida Ribeiro Carvalho, M.; Botero, W.G.; de Oliveira, L.C. Natural and anthropogenic sources of potentially toxic elements to aquatic environment: A systematic literature review. *Environ. Sci. Pollut. Res.* **2022**, *29*, 51318–51338. [CrossRef]
4. Charkiewicz, A.E.; Omeljaniuk, W.J.; Nowak, K.; Garley, M.; Nikliński, J. Cadmium toxicity and health effects—A brief summary. *Molecules* **2023**, *28*, 6620. [CrossRef]
5. Khan, Z.; Elahi, A.; Bukhari, D.A.; Rehman, A. Cadmium sources, toxicity, resistance and removal by microorganisms—A potential strategy for cadmium eradication. *J. Saudi Chem. Soc.* **2022**, *26*, 101569. [CrossRef]
6. Abd Elnabi, M.K.; Elkaliny, N.E.; Elyazied, M.M.; Azab, S.H.; Elkhalifa, S.A.; Elmasry, S.; Mouhamed, M.S.; Shalamesh, E.M.; Alhorieny, N.A.; Abd Elaty, A.E.; et al. Toxicity of heavy metals and recent advances in their removal: A Review. *Toxics* **2023**, *11*, 580. [CrossRef]
7. Ojha, N.; Karn, R.; Abbas, S.; Bhugra, S. Bioremediation of industrial wastewater: A review. *IOP Conf. Ser. Earth Environ. Sci.* **2021**, *796*, 012012. [CrossRef]

8. Priyadarshanee, M.; Das, S. Biosorption and removal of toxic heavy metals by metal tolerating bacteria for bioremediation of metal contamination: A comprehensive review. *J. Environ. Chem. Eng.* **2021**, *9*, 104686. [CrossRef]
9. Bahafid, W.; Joutey, N.T.; Asri, M.; Sayel, H.; Tirry, N.; Ghachtouli, N.E. Yeast biomass: An alternative for bioremediation of heavy metals. In *Yeast—Industrial Applications*; IntechOpen: London, UK, 2017. [CrossRef]
10. Ciani, M.; Adessi, A. Cyanoremediation and phyconanotechnology: Cyanobacteria for metal biosorption toward a circular economy. *Front. Microbiol.* **2023**, *14*, 1166612. [CrossRef]
11. Rajput, A.P.; Kulkarni, M.; Pingale, P.L.; Tekade, M.; Shakya, A.K.; Tekade, R.K. Chapter 16—Understanding the bioaccumulation of pharmaceuticals and personal care products. In *Essentials of Pharmatoxicology in Drug Research*; Elsevier: Amsterdam, The Netherlands, 2023; Volume 1, pp. 393–434. [CrossRef]
12. Saleh, H.E.-D.M.; Aglan, R.F. (Eds.) *Heavy Metals*; InTech: London, UK, 2018. [CrossRef]
13. Raji, Z.; Karim, A.; Karam, A.; Khalloufi, S. Adsorption of heavy metals: Mechanisms, kinetics, and applications of various adsorbents in wastewater remediation—A Review. *Waste* **2023**, *1*, 775–805. [CrossRef]
14. Hamidu, I.; Afotey, B.; Kwakye-Awuah, B.; Anang, D.A. Synthesis of silica and silicon from rice husk feedstock: A review. *Heliyon* **2025**, *11*, e42491. [CrossRef]
15. Roșca, M.; Diaconu, M.; Hlihor, R.; Cozma, P.; Silva, B.; Tavares, T.; Gavrilescu, M. Evaluation of microbial biosorbents for efficient Cd(II) removal from aqueous solutions. *Water* **2024**, *16*, 3660. [CrossRef]
16. Wang, T.; Zhang, L.; Li, S.; Meng, L.; Su, M.; Wang, Z.; Nong, Y.; Sun, Y.; Wang, S.; Li, Z. Weakened Cd toxicity to fungi under coexistence of Pb in solution. *J. Hazard. Mater.* **2021**, *426*, 127984. [CrossRef]
17. Martini, E.; Andriani, D.; GobiKrishnan, S.; Kang, K.E.; Bark, S.-T.; Sunwoo, C.; Prasetya, B.; Park, D.-H. Immobilization of *Saccharomyces cerevisiae* in rice hulls for ethanol production. *Makara J. Technol.* **2010**, *14*, 150243. [CrossRef]
18. Yu, J.; Zhang, X.; Tan, T. An novel immobilization method of *Saccharomyces cerevisiae* to sorghum bagasse for ethanol production. *J. Biotechnol.* **2007**, *129*, 415–420. [CrossRef]
19. Din, M.I.; Mujahid, A.; Bock, U.; Khalid, R.; Hussain, Z. A kinetic and thermodynamic investigation for adsorption of cadmium (ii) ions on the microwave modified sugar cane bagasse. *Desalin. Water Treat.* **2024**, *317*, 100194. [CrossRef]
20. Tayyab, M.; Anwar, S.; Shafiq, F.; Shafique, U.; Kaya, C.; Ashraf, M. Adsorption isotherms and removal of lead (II) and cadmium (II) from aqueous media using nanobiochar and rice husk. *Int. J. Phytoremediation* **2025**, *27*, 244–259. [CrossRef]
21. McCabe, W.L.; Smith, J.C.; Harriott, P. *Operaciones unitarias en ingeniería química*, 7th ed.; McGraw-Hill: New York, NY, USA, 1998.
22. Kalam, S.; Abu-Khamsin, S.A.; Kamal, M.S.; Patil, S. Surfactant Adsorption Isotherms: A Review. *ACS Omega* **2021**, *6*, 32342–32348. [CrossRef]
23. Gupta, A.; Sharma, V.; Sharma, K.; Kumar, V.; Choudhary, S.; Mankotia, P.; Kumar, B.; Mishra, H.; Moulick, A.; Ekielski, A.; et al. A Review of adsorbents for heavy metal decontamination: Growing approach to wastewater treatment. *Materials* **2021**, *14*, 4702. [CrossRef]
24. De Vargas Brião, G.; Hashim, M.A.; Chu, K.H. The Sips isotherm equation: Often used and sometimes misused. *Sep. Sci. Technol.* **2023**, *58*, 884–892. [CrossRef]
25. Danat, B.T.; Wuana, R.A.; Chahul, H.F.; Iorungwa, M.S. Review of adsorption isotherms models. *Appl. Water Sci.* **2026**, *16*, 72. [CrossRef]
26. Molebatsi, M.; Nkoane, B.; Keroletswe, N.; Chigome, S.; Kabomo, M.T. The use of biosorbents in water treatment. *Environments* **2025**, *12*, 302. [CrossRef]
27. Sukmana, H.; Radojčin, M.; Gyulavári, T.; Kozma, G.; Kónya, Z.; Hodúr, C. Utilization of rice husks as effective bioadsorbents for methylene blue removal from wastewater: Characterization, adsorption performance, and regeneration studies. *Appl. Water Sci.* **2025**, *15*, 148. [CrossRef]
28. Yefremova, S.; Kablanbekov, A.; Satbaev, B.; Zharmenov, A. Rice husk-based adsorbents for removal of metals from aqueous solutions. *Materials* **2023**, *16*, 7353. [CrossRef]
29. Cha, H.-G.; Kim, Y.-O.; Choi, W.Y.; Kang, D.-H.; Lee, H.-Y.; Jung, K.-H. Evaluating carriers for immobilizing *Saccharomyces cerevisiae* for ethanol production in a continuous column reactor. *Mycobiology* **2014**, *42*, 249–255. [CrossRef]
30. Xue, S.; Guo, H.; Li, Y.; Dong, N.; Dai, Y.; Ji, C.; Zhu, B.; Zhang, S. Immobilized *Rhodotorula mucilaginosa* DL-XSY01 with electrospinning for ethyl carbamate degradation and flavor preservation in Chinese Baijiu. *Food Biosci.* **2025**, *64*, 105858. [CrossRef]
31. Mussagy, C.U.; Ribeiro, H.F.; Pereira, J.F.B. *Rhodotorula* sp. As a cell factory for production of valuable biomolecules. In *Advances in Applied Microbiology*; Academic Press: Cambridge, MA, USA, 2023; Volume 123, pp. 133–156. [CrossRef]
32. Flores-Trujillo, A.K.I.; Morales-Mendoza, A.G.; Rodríguez-Vázquez, R. Behavior of a mixture of metals for competiting adsorption sites of untreated and alkali-treated rice husk. *Processes* **2024**, *12*, 1299. [CrossRef]
33. Fu, H.; Wang, S.; Zhang, H.; Dai, Z.; He, G.; Li, G.; Ding, D. Remediation of uranium-contaminated acidic red soil by rice husk biochar. *Environ. Sci. Pollut. Res.* **2022**, *29*, 77839–77850. [CrossRef]

34. Lazzari, L.K.; Zimmermann, M.V.G.; Perondi, D.; Zampieri, V.B.; Zattera, A.J.; Santana, R.M.C. Production of Carbon Foams from Rice Husk. *Mater. Res.* **2019**, *22*, e20190427. [CrossRef]
35. Abin-Bazaine, A.A.; Olmos-Marquez, M.A.; Campos-Trujillo, A.A. Fixed-Bed column sorption: Breakthrough curves modeling. In *Sorption—New Perspectives and Applications*; IntechOpen: London, UK, 2024. [CrossRef]
36. Montalvo-Andía, J.; Reátegui-Romero, W.; Peña-Contreraras, A.D.; Zaldivar Alvarez, W.F.; King-Santos, M.E.; Fernández-Guzmán, V.; Guerrero-Guevara, J.L.; Puris-Naupay, J.E. Adsorption of Cd (II) using chemically modified rice husk: Characterization, equilibrium, and kinetic studies. *Adsorpt. Sci. Technol.* **2022**, *2022*, 3688155. [CrossRef]
37. Nemah, A.K.; Naife, T.M. Removal of environmentally polluting heavy metal ions from industrial wastewater using rice husk. In *Advanced Studies on Environmental Sustainability*; Obaid, A.J., Al-Heety, E.A., Radwan, N., Polkowski, Z., Eds.; Springer Nature: Cham, Switzerland, 2024; pp. 167–182. [CrossRef]
38. Gao, Y.; Yi, Z.; Wang, J.; Ding, F.; Fang, Y.; Du, A.; Jiang, Y.; Zhao, H.; Jin, Y. Interpretation of the adsorption process of toxic Cd^{2+} removal by modified sweet potato residue. *RSC Adv.* **2024**, *14*, 433–444. [CrossRef]
39. Zhang, Q.; Chu, R.; Wei, Y.; Lu, Q.; Cai, L. Cadmium adsorption onto aluminum hydroxide-modified attapulgite prepared with basic aluminum acetate. *Sci. Rep.* **2024**, *14*, 31428. [CrossRef]
40. Cecire, R.; Diana, A.; Giacomino, A.; Abollino, O.; Inaudi, P.; Favilli, L.; Bertinetti, S.; Cavalera, S.; Celi, L.; Malandrino, M. Rice husk as a sustainable amendment for heavy metal immobilization in contaminated soils: A pathway to environmental remediation. *Toxics* **2024**, *12*, 790. [CrossRef]
41. Gkika, D.A.; Mitropoulos, A.C.; Kyzas, G.Z. Why reuse spent adsorbents? The latest challenges and limitations. *Sci. Total Environ.* **2022**, *822*, 153612. [CrossRef]
42. Koippully, S.; Nair, V. Developing a biocatalyst showcasing the synergistic effect of rice husk biochar and bacterial cells for the removal of heavy metals. *New J. Chem.* **2023**, *47*, 21199–21213. [CrossRef]
43. Medina-Acevedo, V.d.M. Remoción de plomo y cadmio mediante fibras de *Agave angustifolia* y un consorcio bacteriano como una alternativa de biorremediación. Bachelor's Thesis, Universidad Autónoma del Estado de Morelos, Cuernavaca, Mexico, 2020.
44. Ali, E.A.M.; Sayed, M.A.; Abdel-Rahman, T.M.A.; Hussein, R. Fungal remediation of Cd (II) from wastewater using immobilization techniques. *RSC Adv.* **2021**, *11*, 4853–4863. [CrossRef]
45. Wei, C.; Luo, J.; Hong, W.; He, L.; Zhang, X.; Fan, T. Adsorption performance and mechanism of modified rice hull biochar for lead and cadmium removal in single and competitive systems. *BMC Chem.* **2026**, *20*, 106. [CrossRef]
46. Et-Tanteny, R.; Allaoui, I.; Manssouri, I.; El Amrani, B.; Draoui, K. Kinetic and isotherm studies of nickel and cadmium ions adsorption onto Clay-Chitosan composite. *Results Chem.* **2025**, *13*, 102056. [CrossRef]
47. Quintelas, C.; Rocha, Z.; Silva, B.; Fonseca, B.; Figueiredo, H.; Tavares, T. Biosorptive performance of an *Escherichia coli* biofilm supported on zeolite NaY for the removal of Cr (VI), Cd (II), Fe (III) and Ni (II). *Chem. Eng. J.* **2009**, *152*, 110–115. [CrossRef]
48. Shen, Y.; Li, H.; Zhu, W.; Ho, S.H.; Yuan, W.; Chen, J.; Xie, Y. Microalgal-biochar immobilized complex: A novel efficient biosorbent for cadmium removal from aqueous solution. *Bioresour. Technol.* **2017**, *244*, 1031–1038. [CrossRef]
49. Hegazy, G.E.; Soliman, N.A.; Ossman, M.E.; Abdel-Fattah, Y.R.; Moawad, M.N. Isotherm and kinetic studies of cadmium biosorption and its adsorption behaviour in multi-metals solution using dead and immobilized archaeal cells. *Sci. Rep.* **2023**, *13*, 2550. [CrossRef]
50. Plöhn, M.; Escudero-Oñate, C.; Funk, C. Biosorption of Cd(II) by Nordic microalgae: Tolerance, kinetics and equilibrium studies. *Algal Res.* **2021**, *59*, 102471. [CrossRef]
51. Wang, J.; Guo, X. Adsorption kinetics and isotherm models of heavy metals by various adsorbents: An overview. *Crit. Rev. Environ. Sci. Technol.* **2023**, *53*, 1837–1865. [CrossRef]
52. Fadl, M.G. Prediction of heavy metal biosorption mechanism through studying isotherm kinetic equations. *Sci. Rep.* **2023**, *13*, 1576. [CrossRef]
53. Klein, J.; Ziehr, H. Immobilization of microbial cells by adsorption. *J. Biotechnol.* **1990**, *16*, 1–15. [CrossRef]
54. Velkova, Z.; Kirova, G.; Stoytcheva, M.; Kostadinova, S.; Todorova, K.; Gochev, V. Immobilized microbial biosorbents for heavy metals removal. *Eng. Life Sci.* **2018**, *18*, 871–881. [CrossRef]
55. Shao, Q.; Yan, S.; Sun, X.; Chen, H.; Lu, Y.; Li, S.; Huang, Y.; Wang, S.; Zhang, M.; Li, Z. Applications of yeasts in heavy metal remediation. *Fermentation* **2025**, *11*, 236. [CrossRef]
56. Deng, W.; Mo, Q.; Wei, Z.; Guo, Y.; Liu, J.; Xue, W.; Liu, Y.; Zeng, Z.; Su, Y.; Lu, S. Biological remediation mechanism and applications of *Rhodotorula mucilaginosa* for heavy metal pollution. *Environ. Technol. Innov.* **2025**, *38*, 104179. [CrossRef]

Disclaimer/Publisher's Note: The statements, opinions and data contained in all publications are solely those of the individual author(s) and contributor(s) and not of MDPI and/or the editor(s). MDPI and/or the editor(s) disclaim responsibility for any injury to people or property resulting from any ideas, methods, instructions or products referred to in the content.